Isolated Three-Phase Rectifier Using a Sepic DC-DC Converter in Continuous Conduction Mode For Power Factor Correction

DENIZAR CRUZ MARTINS and ANDERSON H. de OLIVEIRA
Federal University of Santa Catarina - Power Electronics Institute
PO Box 5119 - 88.040-970 - Florianópolis - SC
BRAZIL

Abstract: - This paper presents an analysis of a three-phase rectifier with high power factor using a Sepic DC-DC converter operating in continuous conduction mode (CCM). The structure is particularly simple and robust. Its main features are: one power processing stage, which can operate as step-down or step-up voltage, lower harmonic distortion in the line current and natural isolation. The converter works with constant frequency and PWM modulation. A study for steady state conditions, a design procedure, and experimental results obtained from a laboratory prototype are presented.

Key-Words: - Three-Phase Rectifier, Sepic DC-DC Converter, Power Factor Correction.

1 Introduction

Three-phase feeding systems, available in industrial applications, are usually indicated for high-power systems (over 1kW), where conventional diode and thyristor-controlled rectifiers have dominated AC/DC conversion. The non-linear characteristic of the input current of these rectifiers creates problems for the commercial electric power network, among them the following items can be pointed out: increase of losses in the distribution and transmission lines of the power network, reduction of power factor, need to generate large quantities of reactive power, electromagnetic interference in control and communication system, distortion of the input voltage, and the decrease of the structure efficiency, due to high RMS of the input current.

The scientific community has presented many studies in order to provide the utilization of AC/DC converters with high power factor for the AC network and low harmonic distortion in the input line current [1-7]. One of the most employed topologies, as a pre-regulator, is the Boost converter [1, 2]. This structure is not naturally isolated; it operates only as step-up voltage, and works in discontinuous conduction mode (DCM). The converter proposed in [2] has a good performance, but the structure consists of three synchronized switches, three Y-connected Buck-Boost inductors and another complementary switch to control the output DC voltage. Moreover, the converter is operated in DCM with high RMS current value. In [4] the main advantages of the scheme are the simplicity and the good performance on the AC side; however, the converter works in DCM, and presents a high switch stress. The works shown in [5, 6] are very interesting, and they present a constant power flux. However, the drive and control circuit are complex and the energy transference is still carried out in two stages. The converters are not independent and, for this reason, the reliability of the system is jeopardized. In [7] better results were obtained in terms of the efficiency of the system, operating with constant power flux, but there is still great difficulty on the level of drive circuit implementation due to their complexity and two-stage energy transference.

In this paper, we present an analysis and development of a three-phase input feeding source, high power factor, operating at constant frequency, with a single stage of a power processing, employing the DC/DC Sepic converter (Single Ended Primary Inductance Converter) operating in continuous conduction mode. The structure proposed is naturally isolated, and utilizes only one switch for controlling power flux, making the drive circuit extremely simple, with no need for line filters between the input network and the rectifier, and can operate as step-down or step-up voltage. Furthermore, the reduced number of components increases the reliability of the system, making it quite attractive for industrial applications.

2 Principle of Operation

The proposed circuit is shown in Fig. 1.To simplify the analysis, the following assumptions are made: the operation of the circuit is steady-state, the semiconductors are considered ideal, the transformer is

represented by its magnetizing inductance reflected to the primary side, the voltage ripple across the capacitors C_1 and C_o are considered zero, the line voltage is constant during a switching period and the efficiency of the structure is considered equal to 100%.

By referring the parameters of the converter to the primary side of the transformer we obtain the equivalent circuit shown in Fig. 2, where:

$$R_0 = \left(\frac{N_P}{N_S}\right)^2 \cdot R_0' \; ; \; C_0 = \left(\frac{N_S}{N_P}\right)^2 \cdot C_0' \; ; \; V_0 = \frac{N_P}{N_S} \cdot V_0' \quad (1)$$

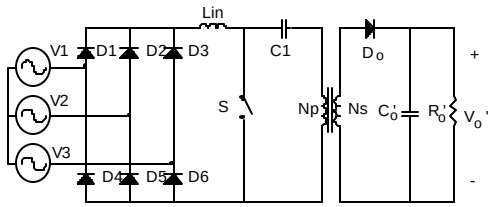

Fig. 1: Proposed circuit

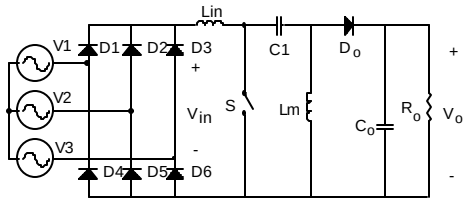

Fig. 2: Equivalent circuit with the parameters referred to the primary side.

The Sepic converter working in continuous conduction mode presents two operation stages:

1st Stage (0<t<DT) Fig. 3: At the moment t = 0, switch S is turned on. The energy from the source V_{in} is stored in the inductance L_{in}, and the capacitor C_1 transfer its energy to the magnetizing inductance L_m. The voltage of the capacitor C_1 is considered constant and equal to V_{in}. The currents i_{in} and i_{Lm} increase linearly. During this stage the diode D_0 is kept blocked and the capacitor C_0 supplies energy to the load R_0.

2nd Stage (DT < t < T)Fig. 4: At the moment t = DT, switch S is turned off and the diode D_0 is turned on, transferring the inductor storage energy to the load. The currents i_{in} and i_{Lm} decrease linearly. The voltage across the switch S is equal to $(V_{in}+V_0)$.

The main waveforms are shown in Fig. 5.

3 Mathematical Analysis

The equations for the functioning of the steady-state Sepic converter operating in CCM are given below:

$$i_{in}(t) = \begin{cases} I_{in_0} + \frac{V_{in}}{L_{in}} \cdot t & ; \; 0 < t < DT \\ \frac{V_{in}}{L_{in}} \cdot DT - \frac{V_0}{L_{in}}(t - DT) + I_{in_0} & ; \; DT < t < T \end{cases} \quad (2)$$

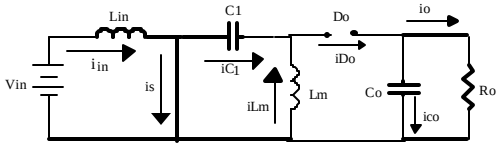

Fig. 3: First stage

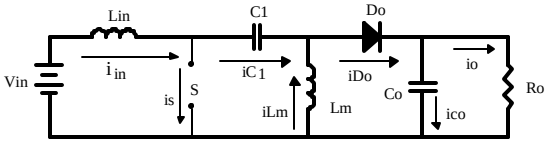

Fig. 4: Second stage

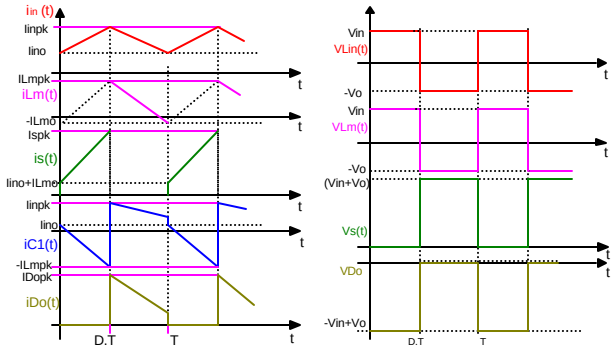

Fig. 5: Main waveforms

$$i_{Lm}(t) = \begin{cases} I_{Lm_0} + \frac{V_{in}}{L_m} \cdot t & ; \; 0 < t < DT \\ \frac{V_{in}}{L_m} \cdot DT - \frac{V_0}{L_m}(t - DT) + I_{Lm_0} & ; \; DT < t < T \end{cases} \quad (3)$$

$$i_S(t) = \begin{cases} \frac{V_{in}}{L_{eq}} \cdot t + I_{in_0} + I_{Lm_0} & ; \; 0 < t < DT \\ 0 & ; \; DT < t < T \end{cases} \quad (4)$$

$$i_{C_1}(t) = \begin{cases} -\frac{V_{in}}{L_m} \cdot t - I_{Lm_0} & ;0 < t < DT \\ \frac{V_{in}}{L_{in}} \cdot DT - \frac{V_0}{L_{in}}(t - DT) + I_{in_0} & ;DT < t < T \end{cases} \quad (5)$$

$$i_{D_0}(t) = \begin{cases} 0 & ;0 < t < DT \\ \frac{V_{in}}{L_{eq}} \cdot DT - \frac{V_0}{L_{eq}}(t - DT) + I_{in_0} + I_{Lm_0} & ;DT < t < T \end{cases} \quad (6)$$

$$V_{L_{in}}(t),\ V_{L_m}(t) = \begin{cases} V_{in} & ;\ 0 < t < DT \\ -V_0 & ;\ DT < t < T \end{cases} \quad (7)$$

$$V_S(t) = \begin{cases} 0 & ;\ 0 < t < DT \\ V_{in} + V_0 & ;\ DT < t < T \end{cases} \quad (8)$$

$$V_{D_0}(t) = \begin{cases} -(V_{in} + V_0) & ;\ 0 < t < DT \\ 0 & ;\ DT < t < T \end{cases} \quad (9)$$

Where: $L_{eq} = \frac{L_{in} \cdot L_m}{L_{in} + L_m}$; $V_{in} = 2.34 \cdot V_{1_{RMS}}$

DT: Switch S_1 conduction time.

From the input current ripple Δi_{in} and the magnetizing current ripple Δi_{Lm} (Fig. 6), the average and the RMS currents through the components of the Sepic converter can be obtained [8]:

* Input and switch average currents:

$$I_{in_{av}} = I_{S_{av}} = \frac{V_{in} \cdot DT}{2 \cdot \overline{\Delta I_{in}} \cdot L_{in}} \quad ; \quad \overline{\Delta I_{in}} = \frac{\Delta I_{in}/2}{I_{in_{av}}} \quad (10)$$

* Average current through the diode "D_0" magnetizing inductance "L_m":

$$I_{D0_{av}} = I_{Lm_{av}} = \frac{V_0 \cdot (1-D) \cdot T}{2 \cdot \overline{\Delta I_{Lm}} \cdot Lm} \ ; \ \overline{\Delta I_{Lm}} = \frac{\Delta I_{Lm}/2}{I_{Lm_{av}}} \quad (11)$$

* Rectifier diodes average current:

$$I_{D_{R_{av}}} = \frac{I_{in_{av}}}{3} \quad (12)$$

* Input RMS current:

$$I_{in_{RMS}} = \frac{\sqrt{3}}{3} \cdot \frac{V_{in} \cdot DT}{2 \cdot \overline{\Delta I_{in}} \cdot L_{in}} \cdot \sqrt{3 + (\overline{\Delta I_{in}})^2} \quad (13)$$

* Switch "S" RMS current:

$$I_{S_{RMS}} = \frac{\sqrt{3}}{3} \frac{V_{in} \cdot DT}{2\overline{\Delta I_{in}} \cdot L_{in}} \cdot \frac{\sqrt{\left[\overline{\Delta I_{in}} \cdot D + \overline{\Delta I_{Lm}}(1-D)\right]^2 + 3}}{\sqrt{D}} \quad (14)$$

* Capacitor "C_1" RMS current:

$$I_{C_{RMS}} = \frac{V_{in} \cdot \sqrt{D} \cdot T}{2 \cdot \overline{\Delta I_{in}} \cdot L_{in}} \cdot \sqrt{\frac{(1-D) \cdot [D \cdot (\overline{\Delta I_{in}})^2 + (1-D) \cdot (\overline{\Delta I_{Lm}})^2 + 3]}{3}} \quad (15)$$

* Diode "D_0" RMS current:

$$I_{D_{0_{RMS}}} = \frac{V_0 \cdot \sqrt{(1-D)} \cdot T}{2 \cdot \sqrt{3} \cdot \overline{\Delta I_{Lm}} \cdot L_m} \cdot \left\{ \sqrt{\left[D \cdot \overline{\Delta I_{in}} + (1-D) \cdot \overline{\Delta I_{Lm}}\right]^2 + 3} \right\} \quad (16)$$

* Capacitor "C_0" RMS current:

$$I_{C_{0_{RMS}}} = \frac{V_0 \cdot (1-D) \cdot T}{2 \cdot \overline{\Delta I_{Lm}} \cdot L_m} \cdot \sqrt{\left\{ \frac{\left[D \cdot \overline{\Delta I_{in}} + (1-D) \cdot \overline{\Delta I_{Lm}}\right]^2 + 3}{3 \cdot (1-D)} \right\} - 1} \quad (17)$$

* Rectifier diodes RMS current:

$$I_{D_{R_{RMS}}} = \frac{\sqrt{3 + (\overline{\Delta I_{in}})^2}}{3} \cdot I_{in_{av}} \quad (18)$$

* Input RMS current:

$$I_{in_{RMS}} = \sqrt{2} \cdot \frac{\sqrt{3 + (\overline{\Delta I_{in}})^2}}{3} \cdot I_{in_{av}} \quad (19)$$

From the conservation of the transformer magnetic flux in steady-state condition, we have:

$$V_{in} \cdot DT = V_0 \cdot (1-D) \cdot T \quad (20)$$

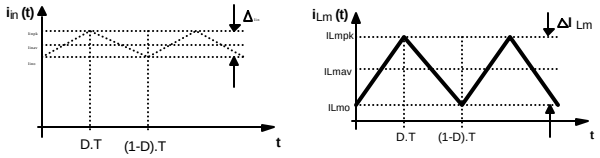

Fig. 6: Input and magnetizing currents of the Sepic Converter.

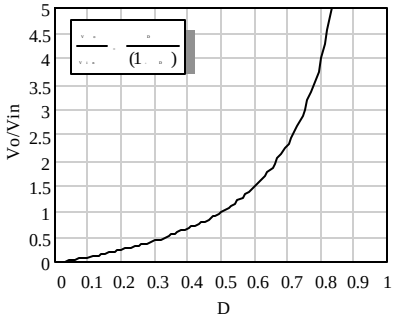

Fig. 7: Static gain.

Thus, the characteristic of the static gain of the Sepic converter in CCM, shown in Fig. 7, is given by:

$$\frac{V_0}{V_{in}} = \frac{D}{(1-D)} \quad (21)$$

Fig. 8 shows the external characteristics of the Sepic converter in steady state [8]. From this figure we can

obtain the current value of the critical load that delimits the continuous and discontinuous modes.

4 Design Procedure and Example

From the equations presented in the previous item, it is possible to generate normalized curves to simplify the converter design. These curves, along with the design procedure, are presented below.

4.1 Input Data

- RMS input phase voltage (V_{RMS} = 220V)
- Output voltage (V_0 = 120V)
- Output power (P_0 = 3.0kW)
- Switching frequency (f_S = 20kHz)
- Normal duty cycle (D = 0.4)
- Efficiency (η = 90%)

4.2 Current Ripple of the Input Inductor ($\overline{\Delta I_{in}}$)

The power factor (PF) and the total harmonic distortion (THD) of the converter input current, are directly affected by the current ripple of the input inductor. Therefore, to obtain a power factor above 95% and a THD near 30%, we must choose a current ripple $\overline{\Delta I_{in}}$ below 10%. In this design it was adopted $\overline{\Delta I_{in}}$ = 2,5% (see Fig. 9 and 10).

4.3 Transformer Ratio (a)

The transformer ratio is given by:

$$a = \frac{V_{in} \cdot D}{V_0 \cdot (1-D)} = \frac{2.34 \cdot 220 \cdot 0.4}{120 \cdot (1-0.4)} \cong 2.86 \qquad (22)$$

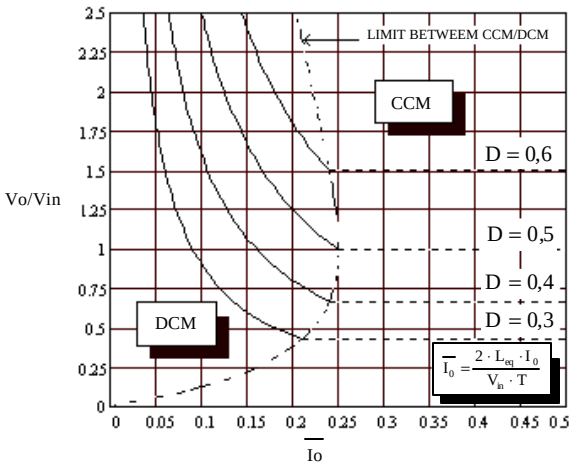

Fig. 8: External characteristics of the Sepic converter.

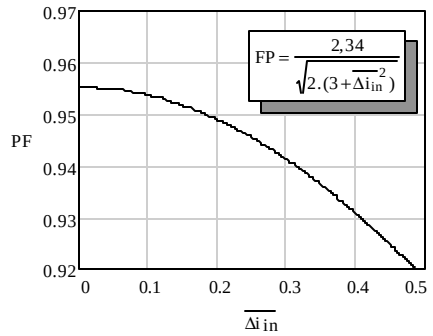

Fig. 9: PF vs. $\overline{\Delta I_{in}}$

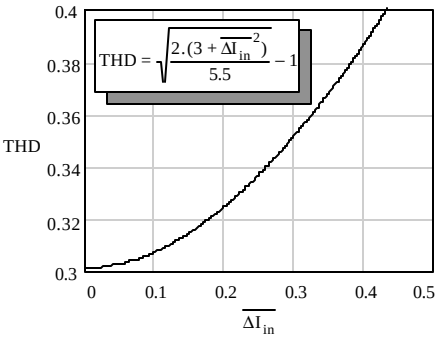

Fig. 10: THD vs. $\overline{\Delta I_{in}}$

4.4 Input Average current ($I_{in_{av}}$)

The input average current is given by the following equation:

$$I_{in_{av}} = \frac{P_0}{\eta \cdot V_{in}} = \frac{3000}{0.9 \cdot 2.34 \cdot 220} \cong 6.5A \qquad (23)$$

4.5 Input Inductor (L_{in})

For that purpose, we adopted 2,5% as input current ripple ($\overline{\Delta I_{in}}$). Therefore:

$$L_{in} = \frac{V_{in} \cdot D}{2 \cdot \overline{\Delta I_{in}} \cdot I_{in_{av}} \cdot f_s} = \frac{2.34 \cdot 220 \cdot 0.4}{2 \cdot 0.025 \cdot 6.5 \cdot 20k} \qquad (24)$$

$$\boxed{L_{in} = 31.68mH}$$

4.6 Equivalent Inductance (L_{eq}) and Magnetizing Inductance (L_m).

For the calculation of the magnetizing inductance, it is necessary to define the maximum load resistence to guarantee the continuous conduction mode of the converter. From Fig. 8 we can observe that the value of the critical normalized load current, for D = 0.4, is approximately equal to 0.24. In the Eq. 25 the value of

$\overline{I_0}$ is adopted to be equal to 6 (six) times the critical normalized load current. Thus, we have:

$$L_{eq} = \frac{V_{in} \cdot V_0 \cdot a \cdot \overline{I_0}}{2 \cdot f_s \cdot P_0} = \frac{2.34 \cdot 220 \cdot 120 \cdot 2.86 \cdot 6 \cdot 0.24}{2 \cdot 20{,}000 \cdot 3{,}000} \quad (25)$$

$$\boxed{L_{eq} = 2.12\text{mH}}$$

From the relation: $L_{eq} = \frac{L_{in} \cdot L_m}{L_{in} + L_m}$; the magnetizing inductance can be obtained:

$$\boxed{L_m = 2.27\text{mH}}$$

4.7 Capacitor C_1 and Output Capacitor (C_0)

For both capacitors a voltage ripple of 1% was adopted. Thus:

$$C_1 = \frac{D^2 \cdot P_0}{\Delta V_{C_1} \cdot (1-D) \cdot V_0^2 \cdot f_s \cdot a^2} = \frac{0.4^2 \cdot 3{,}000}{0.01 \cdot (1-0.4) \cdot 120^2 \cdot 20{,}000 \cdot 2.86^2} \quad (26)$$

$$\boxed{C_1 \cong 33.96\mu\text{F}}$$

$$C_0 = \frac{D^2 \cdot V_{in} \cdot P_0}{\Delta V_{C_0} \cdot V_0^3 \cdot (1-D) \cdot f_s \cdot a} = \frac{0.4^2 \cdot 2.34 \cdot 220 \cdot 3{,}000}{0.01 \cdot 120^3 \cdot (1-0.4) \cdot 20{,}000 \cdot 2.86} \quad (27)$$

$$\boxed{C_2 \cong 417\mu\text{F}}$$

Figs. 11 and 12 show the normalized RMS currents through the capacitors. From Fig. 11 we can obtain the RMS current in the capacitor "C_1", for D = 0.4. The same procedure can be applied for the output capacitor "C_0" from Fig.12. Therefore:

$$I_{C_{1_{RMS}}} = 1.25 \cdot I_{in_{av}} = 1.25 \cdot 6.5 = 8.13\text{A} \quad (28)$$

$$I_{C_{0_{RMS}}} = 0.83 \cdot I_0 = 0.83 \cdot 25 = 20.75\text{A} \quad (29)$$

4.8 Choice of the Semiconductors

From Eqs. (10), (11), (12), (14), (16) and (18), the curves presented in Figs. (13), (14) and (15) can be made. These figures help us in the choice of the semiconductors. Consequently, from Fig. 13, for D = 0.4, the peak and the RMS current through the switches can be obtained.

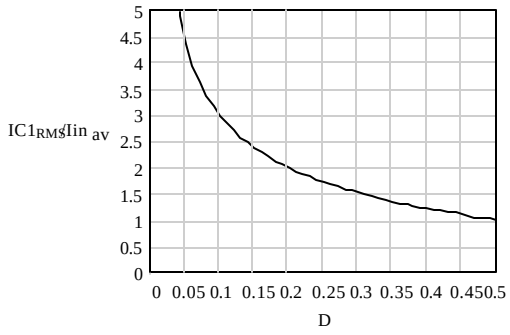

Fig. 11: Normalized RMS current in the capacitor C_1.

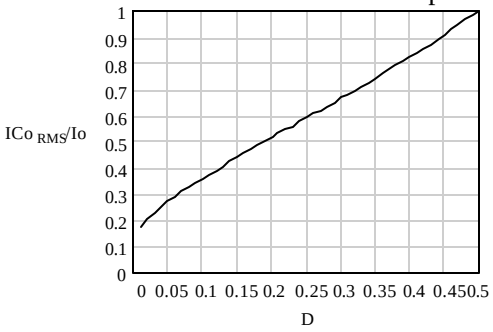

Fig. 12: Normalized RMS current in the capacitor C_0.

$$\begin{cases} I_{S_{PK}} = 3.0 \cdot I_{in_{av}} = 3.0 \cdot 6.5 = 19.5\text{A} & (30) \\ I_{S_{RMS}} = 1.6 \cdot I_{in_{av}} = 1.6 \cdot 6.5 = 10.4\text{A} & (31) \end{cases}$$

By applying the same strategy to Figs. 14 and 15 it is possible to obtain, respectively, the following results:

$$\begin{cases} I_{D_{0_{pk}}} = 1.88 \cdot I_0 = 1.88 \cdot 25 = 47\text{A} & (32) \\ I_{D_{0_{RMS}}} = 1.3 \cdot I_0 = 1.3 \cdot 25 = 32.5\text{A} & (33) \end{cases}$$

$$\begin{cases} I_{DR_{PK}} = 3.1 \cdot I_{DR_{av}} = 3.1 \cdot 2.17 = 6.73\text{A} & (34) \\ I_{DR_{RMS}} = 1.735 \cdot I_{DR_{av}} = 1.735 \cdot 2.17 = 3.76\text{A} & (35) \end{cases}$$

Note: with this design procedure we can obtain all the power circuit components of the three-phase rectifier.

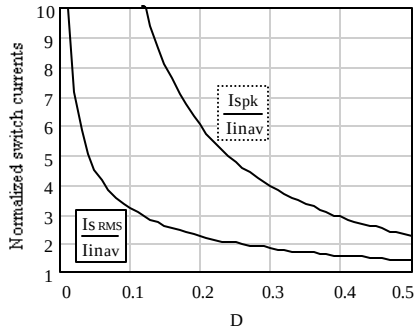

Fig. 13: Peak and RMS normalized current in the switch "S".

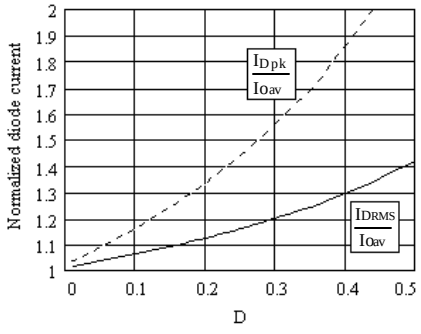

Fig. 14: Peak and RMS normalized current in the diode

"D_0".

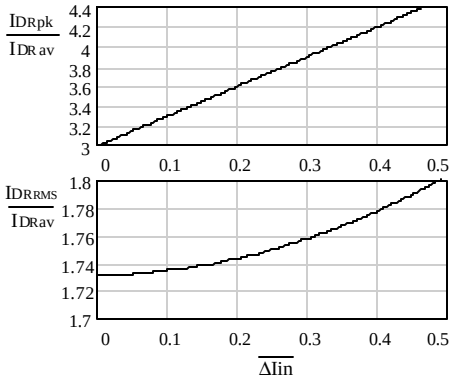

Fig. 15: Peak and RMS normalized current in the rectifier diodes.

5 Experimental Results

A prototype rated 3.0kW was built to evaluate the proposed circuit. The main specifications were given in the previous item. All the results presented in this work were obtained for full load conditions and the output voltage was kept constant, equal to 120V. Fig. 16 shows the voltage and the current of the phase "1". In Fig. 17 it is shown the waveforms of the voltage and the current in the main switch.

Fig. 18 presents the voltage and the current in the diode "D_0". The input inductor current is shown in Fig. 19. The power factor (PF) and the total harmonic distortion (THD) are shown in Figs. 20 and 21, respectively. For the full load conditions the power factor obtained was above 0.96 and the THD was 26%. In the same conditions, the efficiency (η) obtained was about 91% (Fig. 22). The main causes of the losses were: magnetic components, output rectifier and hard switching.

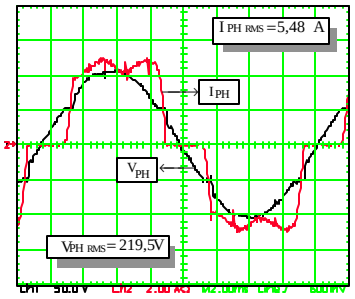

Fig. 16: Voltage and current of phase "1".
Scale: 150V/div; 3A/div; 2ms/div

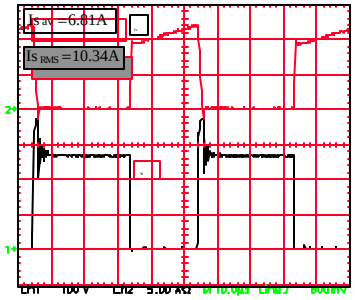

Fig. 17: Voltage and current in the main switch.
Scale: 300V/div; 8A/div; 10µs/div

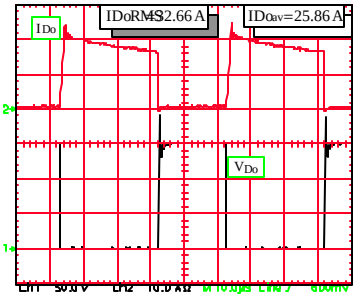

Fig. 18: Voltage and current in the diode "D_0".
Scale: 150V/div; 25A/div; 10µs/div

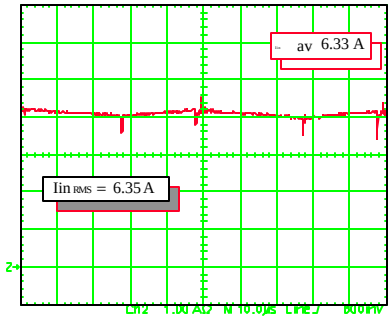

Fig. 19: Input inductor current.
Scale: 1.5A/div; 10µs/div

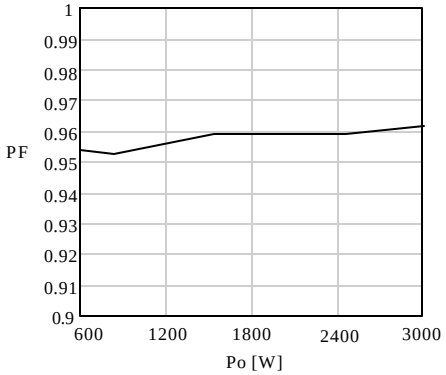

Fig. 20: Power factor behavior.

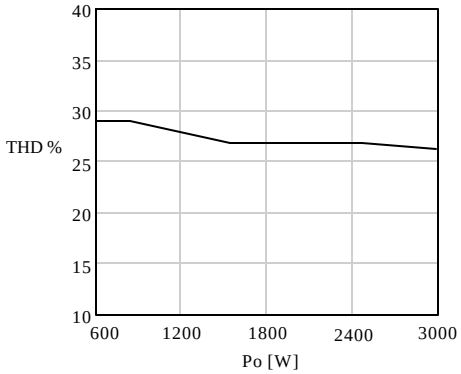

Fig. 21: Total harmonic distortion.

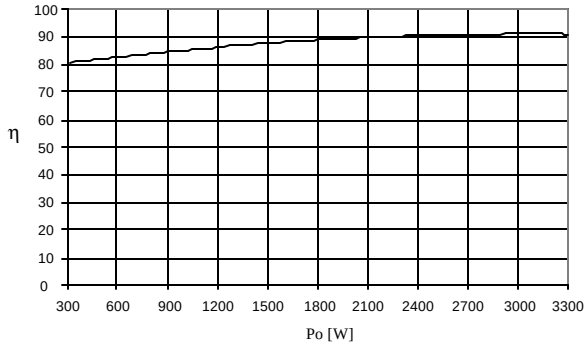

Fig. 22: Efficiency of the prototype.

6 Conclusion

The three-phase rectifier using a Sepic DC-DC Converter has proved to be very robust with easy implementation. The fact that there is only one switch to control the power flux makes a considerably simplified circuit. In the prototype implemented, only one integrator was used to control the static voltage gain. The reduced number of components and the simplicity of its structure increase its reliability and make it extremely desirable for industrial applications.

This structure is particularly used in applications where the load acts as a source voltage. According to the results obtained we have an AC-DC converter with the following features:

- It is particularly simple and robust;
- It provides power factor correction operating in continuous conduction mode and it is therefore more suitable for high power applications;
- It is naturally isolated;
- It has only one controlled switch;
- It operates either as step-up or step-down voltage;
- It can allow a regulated output voltage with only one power processing stage.

Finally, the proposed structure can be utilized at higher power rates without any difficulty.

References

[1] A. R. Prasad, P.D. Ziogas and S. Manias, An Active Power Factor Correction Technique for Three Phase Diode Rectifiers, *Proc. IEEE - PESC'89* , 1989, pp. 58-65.

[2] O. Huang and F. Lee, Harmonic Reduction In a Single Switch Three-Phase Boost Rectifier with Order Harmonic Injected PWM, *in IEEE – PESC'96*, 1996, pp.1266-1271.

[3] C. T. Pan & T.C. Chen, Step-up/down Three Phase AC to DC Converter with Sinusoidal Input Current and Unity Power Factor, *IEEE Proc. Electron. Power Appl.*, Vol. 141, nº 2, 1994, pp. 52-77.

[4] L. Malesani et al, Single-Switch Three-Phase AC/DC Converter with High Power Factor and Wide Regulation Capability, *Proc IEEE - PESC92'*, 1992, pp. 279-285.

[5] B. Ignazia, Unity Power Factor Battery Charger Regulated by LVI, *in Power Quality Proc.*, 1990, pp.42-47.

[6] D. Simonetty, J. Sebastian, and J. Uceda, Single-Switch Three-Phase Power Pre-Regulator Under Variable Switching Frequency and Discontinuous Input Current, *in IEEE-PESC'93 Conf. Rec.*, 1993, pp. 657-661.

[7] J. Pforr and L. Hobson, A Novel Power Factor Corrected Single Ended Resonant Converter With Three Phase Suply, *in IEEE-PESC'92 Conf. Rec.*, 1992, pp. 1369-1375.

[8] A.H. Oliveira, *Three-Phase Rectifier with High Power Factor Using a Continuous Conduction Mode Sepic DC-DC Converter*, Master Thesis, INEP/EEL/UFSC, Florianópolis-SC-Brasil, 1996.